Progress In Electromagnetics Research M, Vol. 70, 41–50, 2018

Design of Compact Lens System for Miniaturized Prolate Spheroidal Impulse Radiating Antenna for Skin Cancer Treatment

Petrishia Arokiasamy*

Abstract—Cancer treatment is one of the several new applications which use subnanosecond pulse and picosecond high voltage pulse. In particular, picosecond pulses can introduce important non-thermal changes in cell biology, especially the permeabilization of the cell membrane. The Prolate Spheroidal Impulse Radiating Antenna (PSIRA) is used to radiate very fast pulses in a narrow beam width with low dispersion and high field amplitude. The beamwidth of the radiated pulse is further reduced by using near field focusing lens. In this proposed work, the compact partition lens system is designed for miniaturized PSIRA to focus the radiated impulse to the target (skin) location. The near field focusing lens is used to enhance the resolution on the target location. The PSR with Modified Bicone Antenna (MBA) with lens configuration provides greatly reduced spot size. The spot size on the target (skin) is measured as 3 mm along the lateral direction and 6 mm along axial direction.

1. INTRODUCTION

Skin cancer is one of the most common forms of cancer. Melanoma is a disease in which malignant (cancer) cells form in melanocytes (cells that color the skin). There are different types of cancer that occur in the skin. Melanoma can occur anywhere on the skin. Unusual moles, exposure to sunlight and health history can increase the risk of melanoma. Signs of melanoma include a change in the way a mole or pigmented area looks. Different treatment methods are implemented to treat skin cancer (melanoma). Recent research shows that intense ultra-short pulses can be used to kill melanoma cells [1]. The effects of intense electric pulses on biological cells provide a new treatment method. Nowadays, needle electrodes are used as a pulse delivery system for treating melanoma. However, this is an invasive approach which leads to discomfort to the patient.

Since the mid-1970s, the development of Electro Magnetic Pulse (EMP) technology provides high power electromagnetic Impulse Radiating Antenna (IRA). The Impulse Radiating Antenna (IRA) is now investigated as a noninvasive subnanosecond pulsed electric field delivery system for skin cancer treatment. The Prolate Spheroidal Impulse Radiating Antenna (PSIRA) is designed for such an application in order to focus the electric field in the near field region where the target (skin) is located. The PSIRA has the advantage of non-invasively delivering the required pulsed electric fields to melanoma cells. It reduces damage to the tissue layers surrounding the target by directly focusing on the target cells. Intense electromagnetic pulses in the subnanosecond range penetrate into living cells to permeabilize intracellular organelles and release Ca^{2+} from the endoplasmic reticulum. Hence, the normal activity of the cell is affected, which leads to cell death [2].

This work deals with a noninvasive, non-thermal therapy using an impulse radiating antenna. The impulse radiating antenna acts as a high power pulsed radiation source for melanoma therapy. For the last few years, several kinds of high power radiation sources have been designed. Currently there appears to be a strong inclination towards compact and autonomous sources of high power microwaves

Received 11 May 2018, Accepted 21 June 2018, Scheduled 2 July 2018
* Corresponding author: Petrishia Arokiasamy (petrishia7@gmail.com).
The author is with the TRP Engineering College, Trichy, Tamil Nadu, India.

Table 1. Existing miniature antenna for high power applications.

S.No	Antenna	Height	Width	Length	Bandwidth Ratio	Ref.
1	Bicone	$\lambda/5$	$\lambda/8.5$	$\lambda/8.3$	5 : 1	[5, 6]
2	Tem Horn	$\lambda/7.5$	$\lambda/7.5$	$\lambda/3.8$	12 : 1	[6]
3	Combined Antenna (Koshelev)	$\lambda/1.5$	$\lambda/1.5$	$\lambda/1.7$	2 : 1	[7, 8]
4	Ridge Horn	$\lambda/7.55$	$\lambda/7.5$	$\lambda/5$	4 : 1	[9]
5	Log periodic	$\lambda/3.9$	$\lambda/150$	$\lambda/3.8$	6 : 1	[5, 6]
6	Valentine	$\lambda/0.9$	$\lambda/5.9$	$\lambda/1.1$	10 : 1	[10, 11]
7	Dragon fly	$\lambda/3.3$	$\lambda/1.28$	λ	12 : 1	[11]
8	Shark	$\lambda/4.4$	$\lambda/4.6$	$\lambda/2.53$	10 : 1	[12]

(HPM). Table 1 shows the existing miniature antennae for high power applications. The antenna for radiating and focusing ultra-wideband and high power signals with low dispersion and high directivity can be a reflector-type antenna or array. Usually an ellipsoidal dish is used. The dish has two focal points. The radiation source is placed at the first focal point, and the target (tumor) is placed at the second focal point. The electric field radiated from the first focal point acts directly on membrane proteins, rather than causing charging of the membrane and if sufficiently strong, can cause direct and instant conformational changes. Subnanosecond pulses (100 ps) are found to alter the cell membrane conductance, and unirectifying channels are formed when cells are exposed to electric field strength on the order of 20 kV/cm for 2000 pulses [3].

In this proposed work, the PSR (Prolate Spheroid Reflector) with Modified Bicone Antenna (MBA) feed configuration is used to radiate subnanosecond pulsed electric field on the target for noninvasive treatment of skin cancer [4]. The PSIRA comprises two parts: Prolate Spheroidal Reflector (PSR) and feed antenna structure. The PSR has two foci. A fast (100 ps) and intense pulse radiated from the first focal point is focused onto a target (skin) located at the second focal point (near field). The main objective of the work is to enhance the spatial resolution on the target by reducing the spot size of the focused electric field at the second focal point. The enhancement of spatial resolution is obtained by using a near field focusing lens system before the target. A compact three-layer lens system is designed for Miniaturized Prolate Spheroidal Impulse Radiating Antenna. The lens system matches the focused electric pulses with the target medium. The spot size is obtained from the numerical calculation of FWHM (Full Width Half Maximum) of the focal waveform.

This paper is organized as follows. In Section 2, the design of Prolate Spheroidal Antenna with Modified Bicone Antenna feed is discussed. Section 3 presents the compact partition lens system. Skin model is discussed in Section 4. Section 5 presents the electromagnetic simulations of antenna with lens and target.

2. PROLATE SPHEROIDAL REFLECTOR WITH MODIFIED BICONE ANTENNA FEED

2.1. Prolate Spheroidal Reflector (PSR) Design

The Impulse Radiating Antenna (IRA) consists of three elements: a Prolate Spheroidal Reflector, a miniature feed structure and feeding mechanism. The schematic diagram of Prolate Spheroidal Reflector is shown in Figure 1. The reflector semi-major axis (a) is 120 mm. The semi-minor axis (b) is 100 mm. It has two foci. The focal distance $z_0 = \sqrt{a^2 - b^2}$, i.e., 66.33 mm. The second focal point is close to the near field region with focal distance less than $2D^2/\lambda$, where D is the aperture diameter, and λ is the wavelength. The second focal point is 186 mm from the vertex of the reflector where the skin is exposed. The proposed dimensions of the reflector are minimized as compared to the traditional PSR [13].

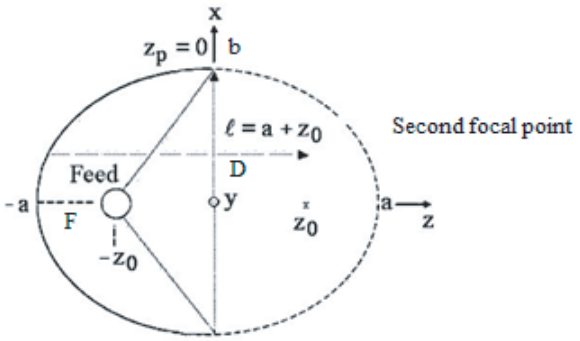

Figure 1. Schematic diagram of Prolate Spheroidal Reflector with geometric parameter.

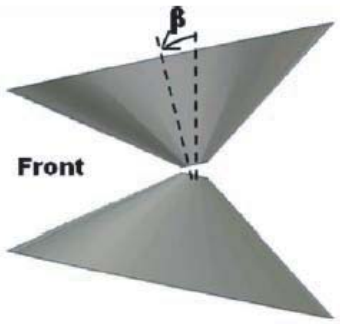

Figure 2. Bicone antenna with slant angle $\beta = 17°$.

2.2. Modified Bicone Antenna Feed Design for PSR

The most important design of Prolate Spheroidal Impulse Radiating Antenna (PSIRA) is its feed antenna design. This section discusses the design of a UWB antenna feed which is miniaturized with respect to overall dimensions of the system and is able to radiate with high gain, high electric field intensity transient pulses at high repetition rates. The MBA feed is designed for Prolate Spheroidal Reflector. It is very suitable for UWB applications such as high power subnanosecond pulse radiation. It is a miniature feed element. The height and width are lower than $\lambda/4$. It has high directivity and high gain. The array structure of MBA elements provides the spot beam radiation which is suitable for cancer therapy, where it reduces the damage of healthy tissues.

The design of MBA is begun with Bicone Antenna. In order to focus the radiation in one direction, the two cones are slanted in the desired direction. Figure 2 shows the bicone antenna with slant angle β which is equal to 17°. The bicone antenna is used to match a wide band of frequency.

The bicone antenna is reshaped or truncated at the bottom, top, side and rear end of the antenna. The frequency spectrum (2 GHz–30 GHz) is chosen to illustrate the design of this antenna as shown in Figure 3. The dimensions for reshaping the structure of Bicone Antenna are optimized to improve the radiation characteristics and also to design a compact array feed for PSR. The length of the antenna is 24 mm. The height and width are designed as 40 mm and 16.42 mm, respectively. The excitation gap between the cones is optimized as 2 mm.

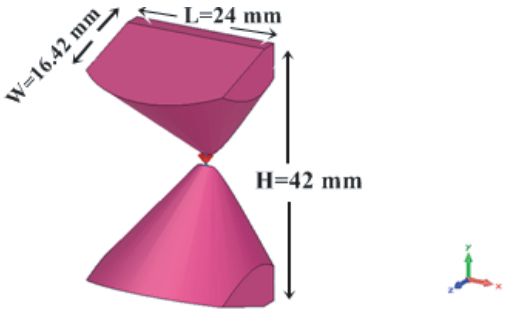

Figure 3. Structure of modified bicone antenna.

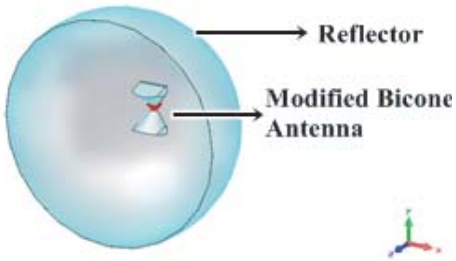

Figure 4. Modified bicone antenna with reflector.

The maximum wavelength of the spectrum that has to be covered is $\lambda_{2\,\mathrm{GHz}} = 150$ mm. The generalized size of the antenna is

- Length 24 mm = $\lambda_{2\,\mathrm{GHz}}/6.25$
- Width 16.42 mm = $\lambda_{2\,\mathrm{GHz}}/9.135$

- Height 40 mm = $\lambda_{2\,\mathrm{GHz}}/3.75$

Thus MBA is miniaturized as far as the width and length are concerned. MBA feed is placed in the first focal point of the Prolate Spheroidal Reflector which is shown in Figure 4. The antenna is excited with 1 V 100 ps rise time ramp rising step signal.

Table 2 shows the radiation characteristics of MBA fed PSR. Figure 5 shows the return loss and VSWR. The return loss is less than −10 dB for the bandwidth of 2–30 GHz. For the entire bandwidth, the VSWR is less than 2.

Table 3 shows the comparison of the proposed feed configuration of Impulse Radiating Antenna

Table 2. Radiation characteristics of MBA FED PSR.

S.No	Radiation Characteristics	MBA FEED
1.	Bandwidth ratio	15 : 1
2.	Directivity (dBi)	19.56
3.	Side lobe level (dB)	−11
4.	3 dB beam width (degree)	12.2
5.	Electric field Intensity (V/m)	74.15
6.	VSWR	< 2 for (2–30 GHz)

Table 3. Comparision between MBA fed PSIRA configurations with existing IRA.

S.No	Features	PSR with Conical Feed	IRA with ACD Feed	IRA with TEM wire Feed	PSR with MBA Feed
1.	Reflector Diameter (cm)	62	46	120	20
2.	Gain (dB)	Traditional IRA-25 Improved IRA-28	−25	28.3	19.56
3.	F/D ratio	0.4	0.39	0.38	0.33
4.	Electric field Intensity (V/m)	5.44 for 1 V i/p	2 for 0.35 V i/p	3 V for 1 V i/p	74.15 for 1 V i/p
5.	VSWR	< 2 for (0.66–19.22 GHz)	< 2 for (0.5–15 GHz)	< 2 for (0.5–5 GHz)	< 2 for 2.45–30 GHz)
	References	[20–22]	[23]	[24]	

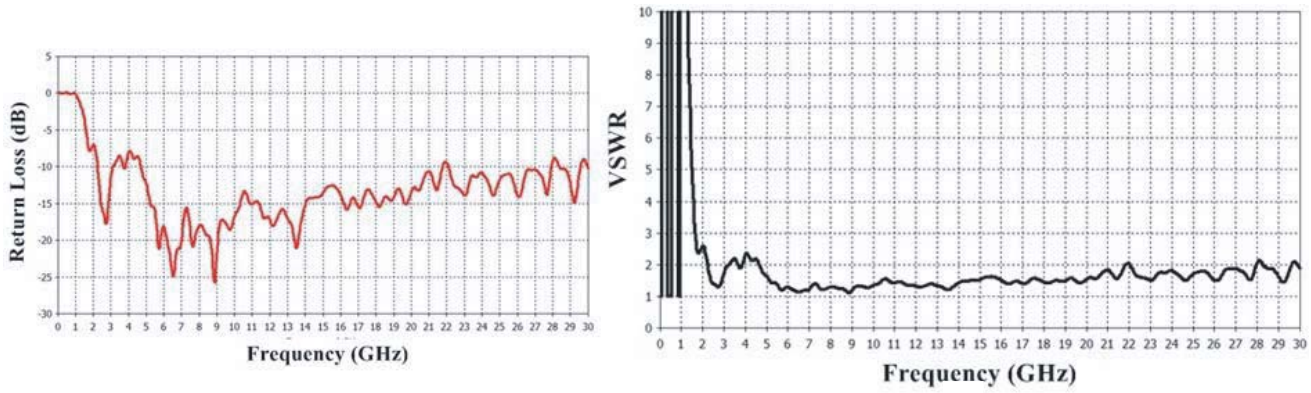

(a) (b)

Figure 5. (a) Return loss in dB and (b) VSWR for MBA fed PSIRA.

with existing feed structures. The conical feed with reflector of 62 cm diameter gives the gain of 28 dB. The radiated field is higher for the proposed configuration. The reflector diameter for MBA fed PSIRA is small compared to the rest of the IRA which provides a moderate gain and wide bandwidth.

3. ANALYTICAL MODEL OF PARTITION LENS SYSTEM

The design of a partition dielectric lens, with relative permittivity of 2, is shown in Figure 6. The partition lens is designed based on Fermat's Aplanatic principle and Fresnel law of refraction [14, 15]. The design contour of each layer is determined from the following equation

$$y_i = f_i(x) = \sqrt{(n^2-1)x^2 - 2n(n-1)Fx + (n-1)^2F^2} \tag{1}$$

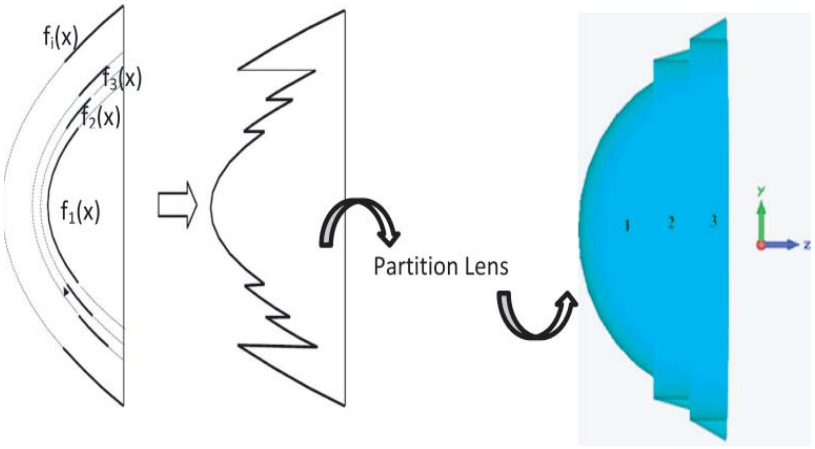

Figure 6. Design of partition lens from hemisphere dielectric lens.

The thickness of the lens is varied from t_i to t_1. The thickness and number of layers are reduced by partitioning the lens. The relative dielectric constant $\varepsilon_r = 2$ for all three layers.

In the lens design, the phase difference between the electromagnetic waves plays an important role. The layers of the lens are designed with different focal lengths and optical paths. The electromagnetic waves through different parts of the lens have different phases. The partition lens is designed such that the phase difference between electromagnetic waves through different parts of the lens is an integer multiple of 2π when they arrive at focal point.

This is a three-layer partition lens system. The number of layers is optimized based on the transmission coefficient of the electromagnetic waves inside the lens layers. The 3-layer lens system provides higher electric field with reduced spot size.

The thickness of the lens can be reduced by uniting lens with different focal lengths. However, here comes another problem that different lenses have different optical paths. The electromagnetic waves through different parts of the lens have different phases. we must make sure that the phase difference between electromagnetic waves through different parts of the lens is an integer multiple of 2π when they arrive at focal point.

Figure 7 shows the optical path length. L_i is the optical path length of electromagnetic waves through the part of the lens,

$$\text{Where} \quad L_i = F_i + n \times t_i \tag{2}$$

$F_i + t_i$ = Constant; n is the refractive index of the lens; F_i is the focal length of the ith layer; t_i = thickness of the ith layer. $L_i > \ldots L_3 > L_2 > L_1$

$$L_i = L_{i-1} + \lambda = L_{i-2} + 2\lambda = L_{i-3} + 3\lambda = L_i = (i-1)\lambda \tag{3}$$

The appropriate focal length for each layer is chosen to make sure that the difference of optical length between the layers is an integer multiple of wavelength (1 cm). The design parameters are shown

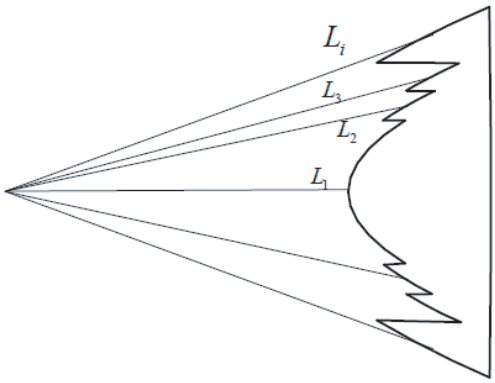

Figure 7. Optical path length of electromagnetic waves through the part of the lens.

in Table 4 for 3 layers. The inner and outer radii are used to decide the area of each layer. This will have effect on the focusing ability of the partition lens. The area of the partition is optimized in order to obtain reduced spot size and enhanced electric field at the second focus. The intensity of the wave decreases from the reflector and increases at the geometric focus. Adding partition lens allows one to increase the field intensity near the geometric focus, but the strongest intensity is still found along the axis and increases as the wave penetrates deeper into the tissue.

Table 4. Design parameter for partition lens.

Parameter	Layer-1	Layer-2	Layer-3
Dielectric constant (ε_r)	**2**	**2**	**2**
Focal Length (cm)	**3**	**2**	**1**
Outer radius (cm)	**4**	**4.5**	**5**
Inner radius (cm)	**0**	**4**	**4.5**

The proposed lens is used to solve the thickness and volume problem of the short focus dielectric lens. The field at the second focus is higher because the phase difference between electromagnetic waves through the different part of the lens is chosen as integer multiples of 2π.

4. SKIN MODEL DESCRIPTION

4.1. Two Layer Skin Model

The skin model chosen in this case has been set up with a specific length and width. This is a two-layer model which consists of the epidermis and dermis with the thickness of 0.15 mm and 3.85 mm, respectively. The length and width of the phantom have been specified by 20 mm × 20 mm. The phantom is kept at the distance of 176 mm from the antenna vertex. The phantom is modeled according to the dielectric properties given in Table 5 [15–19].

Table 5 shows the dielectric properties of skin layers. The dielectric constants for the two layers are the same. The thicknesses of the two layers are different. This is the representation of the two-layer skin model.

No cancer cell model is introduced. In the proposed design, the superficial skin cancer type is concentrated. The superficial cancer affects both the layers. If the cancer cell model is introduced in skin layer, the electric field measured at the tumor area is higher than the rest of the skin area.

Table 5. Dielectric properties of skin model.

S.No	Properties	Epidermis	Dermis
1.	Layer Thickness	0.15 m	3.35 mm
2.	Dielectric constant	38	38
3.	Conductivity (S/m)	0.2	0.2
4.	Material Density (Kg/m^2)	1100	1100
5.	Thermal Conductivity (W/K/m)	0.5	0.5
6.	Heat capacity (KJ/K/kg)	3.35	3.35
7.	Permittivity	1	1

5. RADIATION CHARACTERISTICS OF PSIRA WITH COMPACT LENS SYSTEM

5.1. Electromagnetic Simulation Setup

The miniaturized PSIRA with compact partition lens systems is designed and simulated. The simulation software CST Microwave Studio is used to realize a model of the original antenna. CST MWS is based on the finite integration technique (FIT), a very general approach, which describes Maxwell's equations on a grid space and can be used in time domain as well as infrequency domain. The time-domain solver is used to simulate the whole structure. The simulation setup is shown in Figure 8.

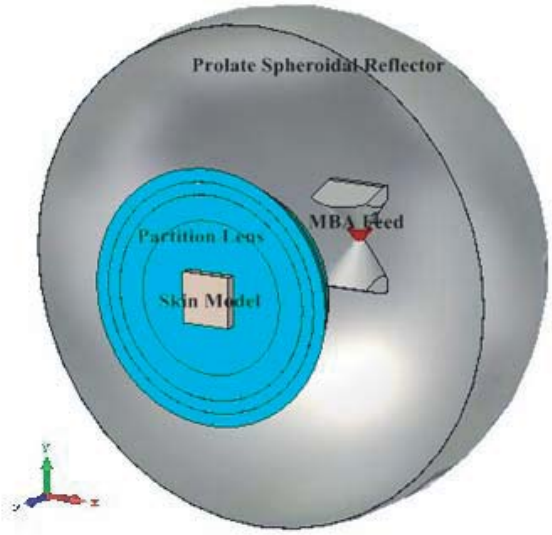

Figure 8. Perspective view of entire simulation setup.

5.2. Electric Field Response at the Focal Point with Skin Layers and Lens

The electric field distribution around the second focal point is shown in Figures 9(a)&(b). The electric fields along lateral direction with and without lens are shown in Figure 9(a). The probes are placed along x-axis, where $x = 0$ corresponds to second focus to measure lateral component of electric field. The peak electric field at the second focus is measured as 170 V/m without lens. The peak enhanced electric field at the second focus is measured as 294 V/m using lens. The FWHM measured along lateral direction is 5 mm without partition lens configuration. The FWHM measured along lateral direction is 3 mm with partition lens configuration. The electric field along axial direction is shown in Figure 9(b).

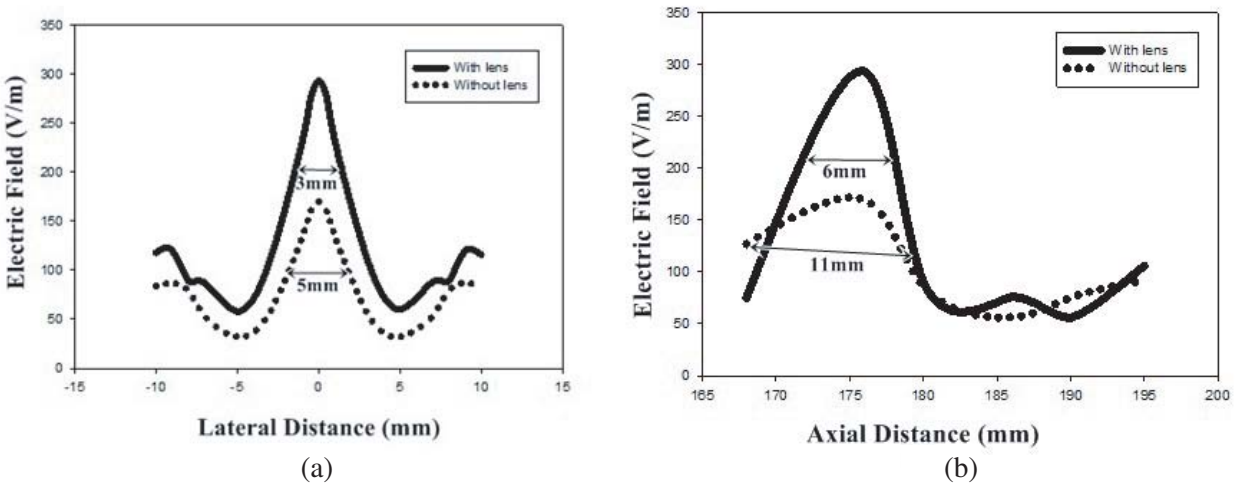

Figure 9. Electric field distribution around second focal point. (a) Electric field PSIRA with compact lens along lateral direction. (b) Electric field distribution PSIRA with compact lens along axial direction.

The probes are placed along z-axis, to measure the axial component of the electric field. The FWHM is measured as 11 mm along axial direction without lens. With lens configuration the spot size is reduced to 6 mm. The miniaturized PSIRA with a compact lens system greatly reduces the spot size along the lateral and axial directions.

The second focal point of the PSIRA is in radiated near field region (Fresnel region). The electric field is measured at the second focal point. It is noted that the maximum of the impulse electric field on the axis is shifted slightly from the geometric focus ($z_o = 66.33$ mm) toward the reflector, which is observed in the modeled result. This is because the impulse decreases inversely with the distance while it is focused in space. At the focal point, even though we have a coherent combination of waves, the impulse electric field is still smaller than the nearby locations toward the reflector due to a large impulse width. In order that the maximum impulse amplitude occurs at the geometric focus, the impulse width needs to be small compared to both $2z_o$ and $2b$. A pulse with faster rise time should allow the shift of the focal spot towards the geometric focus.

6. CONCLUSION

The Prolate Spheroidal Reflector (PSR) with Modified Bicone Antenna (MBA) feed arm with a compact lens system is designed for noninvasive skin cancer treatment. 100 ps electric pulse is launched from the first focal point and is focused at the second focal point where the target is placed. The focal spot is of elliptic shape. The FWHM of Electric field intensity is 3 mm in the axial direction and 6 mm in the lateral direction. The spot size reduction is more beneficial, and it reduces the damage of healthy tissue. The partition lens system is used to reduce the spot size and enhance the electric field at the second focus where the target is placed. Practically high voltage pulse generator becomes technically challenging one. The electric field at the target location is 294 V/m for 1 V input. So the proposed lens system with MBA fed PSIRA reduces the input voltage requirement to obtain high field for the treatment of skin cancer.

REFERENCES

1. Nuccitelli, R., U. Pliquett, X. Chen, W. Ford, J. Swanson, S. J. Beebe, J. F. Kolb, and K. H. Schoenbach, "Nanosecond pulsed electric fields cause melanomas to self-destruct," *Biochemisry Biophysics Res. Commun.*, Vol. 343, No. 2, 351–360, 2006.
2. Schoenbach, K. H., B. Hargrave, R. P. Joshi, J. F. Kolb, C. Osgood, R. Nuccitelli, A. Pakhomov, R. J. Swanson, M. Stacey, J. A. White, S. Xiao, J. Zhang, S. J. Beebe, P. F. Blackmore, and

E. S. Buescher, "Bioelectric effects of intense nanosecond pulses," *IEEE Transacions on Dielectric Electrical Insulation*, Vol. 14, No. 5, 1088–1119, 2007.

3. Schoenbach, K. H., S. Xiao, R. P. Joshi, J. T. Camp, T. Heeren, J. F. Kolb, and S. J. Beebe, "The effect of intense subnanaosecond electrical pulses on biological cells," *IEEE Trans. Plasma Sci.*, Vol. 36, No. 2, 414–422, Apr. 2008.
4. Petrishia, A. and M. Sasikala, "Design of compact electromagnetic impulse radiating antenna for melanoma treatment," *Electromagnetic Biology Medicine*, Vol. 35, No. 2, 134–142, Feb. 2015.
5. Begaud, X., C. Roblin, S. Bories, A. Sibille, and A. C. Lepage, "Antenna design, analysis and numerical modeling for impulse UWB," *WPMC 2004*, Italy, 2004.
6. Ghosh, D., A. De, M. C. Taylor, T. K. Sarkar, M. C. Wicks, and E. L. Mokole, "Transmission and reception by ultra wideband (UWB) antennas," *IEEE Trans. on Antennas and Propagation*, Vol. 48, No. 5, 67–99, 2006.
7. Koshelev, V. I., V. P. Gubanov, A. M. Efremov, S. D. Korovin, B. M. Kovalchuk, V. V. Plisko, A. S. Stepchenko, and K. N. Sukhushin, "High-Power ultrawideband radiation source with multielement array antenna," *13th Int. Symp. on High Current Electronics*, 2004.
8. Andreev, Yu. A., Yu. I. Buyanov, and V. I. Koshelev, "Combined antennas for high-power ultrawideband pulse radiation," *14th Int. Symp. on High Current Electronics*, 2006.
9. Hizal, A. and U. Kazak, "A broadband coaxial ridged horn antenna," *Proc. 19th Eur. Microwave Conf.*, 247–252, 1989.
10. Diot, J. C., P. Delmote, J. Andrieu, M. Lalande, V. Bertrand, B. Jecko, S. Colson, R. Guillerey, and M. Brishoual, "A novel antenna for transient applications in the frequency band 300 MHz–3 GHz: The valentine antenna," *IEEE Trans. on Antennas and Propagation*, Vol. 55, No. 3, 987–990, 2007.
11. Delmote, P., C. Dubois, J. Andrieu, M. Lalande, V. Bertrand, B. Beillard, B. Jecko, T. Largeau, R. Guillerey, and S. Colson, "Two original UWB antennas: The dragonfly antenna and the valentine antenna," *Proc. Radar*, Touldouse, France, 2004.
12. Desrumaux, L., A. Godard, M. Lalande, V. Bertrand, J. Andrieu, and B. Jecko, "An original antenna for transient high power UWB arrays: The shark antenna," *IEEE Trans. on Antennas and Propagation*, Vol. 58, No. 8, 2010.
13. Xiao, S., S. Altunc, P. Kumar, C. E. Baum, and K. H. Schoenbach, "A reflector antenna for focusing in the near field," *IEEE Antennas Wireless Propag. Lett.*, Vol. 9, 12–15, 2010.
14. Nábělek, B., M. Malý, and V. Jirka, "Linear Fresnel lenses, their design and use," *Renewable Energy*, Vol. 1, No. 3–4, 403–408, 1991.
15. Chahat, N., M. Zhadobov, R. Sauleau, and S. I. Alekseev, "New method for determining dielectric properties of skin and phantoms at millimeter waves based on heating kinetics," *IEEE Transactions on Microwave Theory and Techniques*, Vol. 60, No. 3, Mar. 2012.
16. Camp, J. T., Y. Jing, J. Zhuang, J. F. Kolb, S. J. Beebe, J. Song, R. P. Joshi, S. Xiao, and K. H. Schoenbach, "Cell death induced by subnanosecond pulsed electric fields at elevated temperatures," *IEEE Trans. Plasma Sci.*, Vol. 40, No. 10, Oct. 2012.
17. http://niremf.ifac.cnr.it/tissprop.
18. Gustrau, F. and A. Bahr, "W-band investigation of material parameters, SAR distribution, and thermal response in human tissue," *IEEE Transactions on Microwave Theory and Techniques*, Vol. 50, No. 10, Oct. 2002.
19. Garon, E. B., D. Saucer, P. T. Vernier, T. Tang, Y. Sun, L. Marcu, M. A. Gundersen, and H. P. Koeffler, "In vitro and in vivo evaluation and a case report of intense nanosecond pulsed electric field as a local therapy for human malignancies," *Int. J. Cancer*, Vol. 121, No. 3, 675–682, Aug. 2007.
20. Kumar, P., C. E. Baum, S. Altunc, J. Buchenauer, S. Xiao, C. G. Christodoulou, E. Schamiloglu, and K. H. Schoenbach, "Hyperband antenna to launch and focus fast high-voltage pulses onto biological targets," *IEEE Transactions on Microwave Theory and Techniques*, Vol. 59, No. 4, 1090–1101, 2011.

21. Xiao, S., S. Altunc, P. Kumar, C. E. Baum, and K. H. Schoenbach, "A reflector antenna for focusing in the nearfield," *IEEE Antennas Wireless Propag. Lett.*, Vol. 9, 12–15, 2010.
22. Qiu, J., B. S. Zhang, and N. Wang, "Improved design of the reflector impulse radiating antenna," *International conference on Ultrewideband and Ultra-short Impulse Signals*, 15–19, Sevastopol, Ukraine, 2008.
23. Singh, D. K., D. C. Pande, and A. Bhattacharya, "Improved feed design for enhance performance of reflector based impulse radiating antennas," *Sensor and Simulation Notes*, Note 565, 2013.
24. Lee, D., H. Lee, S. Hwang, and J. Ahn, "Design of an impulse radiating antenna using a curved TEM-wire fed parabola," *International Journal of Antennas and Propagation*, Vol. 2012, 2012.